Acta Oceanol. Sin., 2020, Vol. 39, No. 11, P. 103–114
https://doi.org/10.1007/s13131-020-1668-z
http://www.hyxb.org.cn
E-mail: hyxbe@263.net

Physical structure and phytoplankton community off the eastern Hainan coast during summer 2015

Sumin Liu[1, 2, 3], Bo Hong[4*], Guifen Wang[5], Weiqiang Wang[1], Qiang Xie[2, 6], Zekai Ni[2], Liu Yu[2], Huichang Jiang[2], Tong Long[2], Hongzhou Xu[2*]

[1] State Key Laboratory of Tropical Oceanography, South China Sea Institute of Oceanology, Chinese Academy of Sciences, Guangzhou 510301, China

[2] Institute of Deep-sea Science and Engineering, Chinese Academy of Sciences, Sanya 572000, China

[3] Graduate School, University of Chinese Academy of Sciences, Beijing 100049, China

[4] South China University of Technology, Guangzhou 510641, China

[5] Hohai University, Nanjing 210098, China

[6] Center for Ocean Mega-Science, Chinese Academy of Sciences, Qingdao 266071, China

Received 9 May 2020; accepted 31 May 2020

Abstract

Based on satellite remote sensing dataset and survey data during upwelling season of 2015, the spatial structures of phytoplankton biomass and community for the first time in the eastern Hainan upwelling (EHU) and its adjacent area, the eastern Leizhou Peninsula upwelling (ELPU) were illustrated. It is found that a significant cold tongue with high salinity and low temperature along the eastern Hainan coast driven by upwelling-favorable summer monsoon. The ELPU was relative weaker than the EHU because of its wide and gentle continental slope. Due to mixing by tides and waves, DO concentration with high value (>6.0 mg/L) were almost homogenous from surface to 30 m depth at the EHU. Beneath that, low DO water (<6.0 mg/L, anoxia) were pumped upward from bottom by the upwelling. The ELPU has worse DO condition compared with the EHU where bottom DO were lower than 3.5 mg/L owing to abundant DO consumption. The phytoplankton biomass reached maximal value about 1.5 mg/m^3 at 30 m depth layer rather than surface layer at the EHU indicating the impact limit of upwelling on phytoplankton growth and DO distribution. Nourished by rich nutrient input, the phytoplankton biomass at the ELPU were much higher than the EHU where the maximal value can reach about 4.0 mg/m^3. The phytoplankton biomass were reduced to about 0.2–0.3 mg/m^3 at the offshore areas of the EHU and ELPU which were close to the value at open sea. At the inshore of the EHU, the phytoplankton community was dominated by diatom which accounted for about 50% of phytoplankton biomass. And prokaryotes (about 40%), green algae (about 20%) and prochlorococcus (about 20%) became main species at the offshore of the EHU. At the ELPU, diatom accounted for about 80% of phytoplankton biomass followed by green algae, indicating a different ecosystem at this region compared with the EHU.

Key words: eastern Hainan upwelling, cold tongue, dissolved oxygen, phytoplankton community

Citation: Liu Sumin, Hong Bo, Wang Guifen, Wang Weiqiang, Xie Qiang, Ni Zekai, Yu Liu, Jiang Huichang, Long Tong, Xu Hongzhou. 2020. Physical structure and phytoplankton community off the eastern Hainan coast during summer 2015. Acta Oceanologica Sinica, 39(11): 103–114, doi: 10.1007/s13131-020-1668-z

1 Introduction

Oceanic upwelling is a common phenomenon in coastal region which takes deep water with low temperature, high salinity, and rich nutrients to upper layer that impacts carbon cycling, blooms biotic community, and raises fishery production (Smith, 1995; Pauly and Christensen, 1995). It has been found in global coastal areas including the South China Sea (Xie et al., 2003; Gan et al., 2009; Wang et al., 2014; Shu et al., 2018), the Yellow Sea (Lü et al., 2010), the East China Sea (Yang et al., 2013), the California coast (Benson et al., 2002; Du and Peterson, 2018), the Chile coast (Sobarzo et al., 2007), the Baltic Sea (Lehmann and Myrberg, 2008), the Eastern Atlantic coast (Roy and Reason, 2001), and the North Benguela coast (Emeis et al., 2018).

The eastern Hainan upwelling (EHU) is one of the strongest upwelling systems in the northern South China Sea (NSCS) (Wu and Li, 2003). This upwelling occurs in summer driven by Asian summer monsoon (Hong and Li, 1991; Li, 1993; Gan et al., 2009). Its spatial structure and intensity have been identified by many studies. For instance, Han et al. (1990) defined a region below 30 m depth where sea surface temperature (SST) were less than 24.5°C and salinity were higher than 34.3 psu as the upwelling center off the eastern Hainan coast (EHC). Guo et al. (1998) extended the upwelling center to region within 40 km offshore and depth less than 100 m based on 2-D model results. Xu et al. (2013) found the EHU can merge with western Guangdong upwelling system in the subsurface layer based on survey data. More studies revealed

Foundation item: The National Key Research and Development Program of China under contract No. 2018YFC0309800; the National Natural Science Foundation of China under contract Nos 41666001, 41576006, 41976014, 41776045; the Chinese Academy of Sciences Frontier Basic Research Project under contract No. QYJC201910; the Sanya Governmental Academy-Locality S&T Cooperation Program under contract No. 2015YD28.

*Corresponding author, E-mail: bohong@scut.edu.cn; hzxu@idsse.ac.cn

that this upwelling system varied with year by year under impact by climate modulation (Liu et al., 2009; Jing et al., 2011; Su et al., 2013, Xie et al., 2016). And its driven mechanism were discussed extensively (Lü et al., 2008; Jing et al., 2009, 2015; Su et al., 2011; Li et al., 2012; Wang et al., 2015; Lin et al., 2016; Xie et al., 2017).

The influence of upwelling on temporal and spatial distributions of primary production and biotic community were investigated by few observations at the EHU (Deng et al., 1995; Li et al., 2010, 2011; Yin et al., 2011; Xie et al., 2012). Based on *in-situ* observation during 1978–1979, Deng et al. (1995) concluded that the number of phytoplankton achieved maximum value in June when coastal upwelling reached a period of prosperity at the EHU. Jing et al. (2011) analyzed long-term satellite remote sense dataset and found that chlorophyll *a* (Chl *a*) concentration varied inter-annually at the EHU in which it was much higher during 1997–1998 El Niño year when costal upwelling was enhanced significantly. Chen et al. (2016) measured Chl *a* concentration at two continuous stations and partially illustrated spatial variation of Chl *a* distribution at the EHU during summer 2013. However, these studies were unable to give spatial distribution of phytoplankton at the EHU during upwelling season. In addition, previous studies all focused on variation of phytoplankton biomass at the EHU, while its community structure was rarely identified.

The importance of coastal upwelling ecosystem on determining fishery product has been documented by many studies at the EHU and its adjacent upwelling areas. For instance, Deng et al. (1995) compared the biologic and fishery data at the EHC and stated that the high fish catch occurred at the Qionghai upwelling region. Wang and Hu (2017) evaluated the relation between upwelling and fishery resource at the NSCS based on remote sensing dataset and found the consistency of the primary product and fishery resources at the upwelling areas. Hence, it is necessary to find out the phytoplankton biomass and structure for assessing the impact of upwelling ecosystem on fishery in the EHU. To achieve that, we implemented a cruise during summer 2015 and collected high resolution CTD (conductivity-temperature-depth) data and water samples along the EHC. For comparison, the cruise also covered the eastern Leizhou Peninsula upwelling area (called ELPU hereafter). And we used photosynthetic pigment analysis method to identify phytoplankton community at the EHU and ELPU. This paper was organized as follows: The data and method were described in Section 2, hydrologic structure, phytoplankton distribution and its community structure at the EHU and ELPU were illustrated and discussed in Section 3, and discussions were concluded in Section 4 and the Section 5 is the conclusions.

2 Data and method

2.1 *Hydrological data*

The cruise was taken from 29 July to 7 August in 2015, which collected hydrological data by CTD and water samples by manual water sampler at 69 stations in total along 10 transections (northwest-southeast direction) from the eastern Leizhou Peninsula coast (ELPC) to the EHC ranging from 17°30′ to 21°30′N in latitude and from 110° to 112°30′E in longitude (Fig. 1). These transections were designed to be almost perpendicular to coastal isobaths and stopped at 200 m isobaths where is far away from the EHU and ELPU (Jing et al., 2009; Xie et al., 2012). Hydrological data including temperature, salinity, depth, density and dissolved oxygen (DO) were measured by Seabird SBE-25 plus CTD at all casting stations and standardized into 1-m interval in vertical.

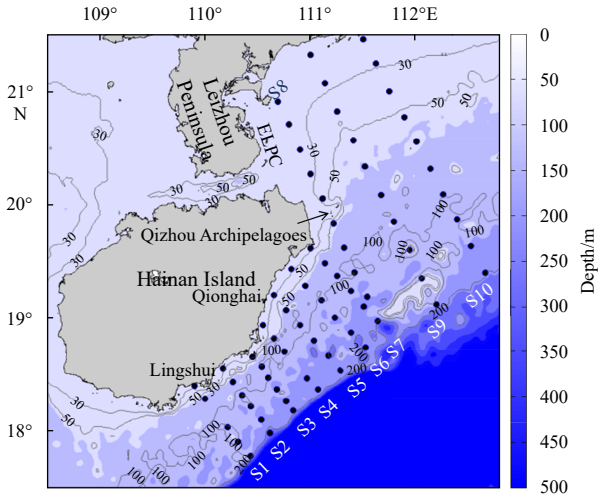

Fig. 1. Topography and sampling station (black dots) along the EHC. Black thin lines represent isobaths (unit: m) and S1–S10 represent 10 survey transections during 2015 cruise.

2.2 *Satellite remote sensing data*

For representing monthly change of hydrologic and phytoplankton characteristics at the EHU during the upwelling season of 2015, the Moderate Resolution Imaging Spectroradiometer (MODIS) monthly averaged sea surface temperature (SST) and Chl *a* concentrations data with 4 km resolution in horizontal from May to September were used in this study (https://oceandata.sci.gsfc.nasa.gov/MODIS-Terra/Mapped/Monthly). The Advanced Scatterometer (ASCAT) monthly and daily averaged wind field data with 0.25°×0.25° resolution in horizontal were used to illustrate external forcing in different time scales at the EHU and ELPU (http://apdrc.soest.hawaii.edu/data/data.php?discipline_index=3). In addition, daily averaged surface level anomaly (SLA) data derived from the AVISO database were used to detect mean dynamic conditions of the EHU and ELPU during the cruise (http://www.aviso.altimetry.fr).

2.3 *Water sample data*

Water samples were collected at standard levels at each station based on water depth (Table 1). Then they were filtered by GF/F filter membrane with 47 mm diameter and 0.7 μm aperture, and the filter membrane were preserved in the liquid nitrogen canister. After the cruise, they were moved into –80°C refrigerator and subjected to the high performance liquid chromatography (HPLC) experiments in the laboratory.

2.4 *Photosynthetic pigment analysis*

To obtain phytoplankton community, we conducted photosynthetic pigment analysis based on HPLC separation methods (van Heukelem and Thomas, 2001). The product model of HPLC analysis system was Waters 1525 Binary HPLC pump and the chromatographic column was Symmetry shields C8 column. We detected the signal with diode array and used two phase gradient elution program in which mobile phase A was the mixture of methanol and 0.5 mol ammonium acetate solution (volume ratio of 70:30 hybrid) and mobile phase B was methanol for HPLC level. Elution gradient was shown in Table 2. We calculated the contents of every pigment (15 pigments in total) according to the peak area of each pigment and its calibration curve, and then gradually transformed them into the concentration of the pigment (Table 3).

Table 1. Water sample standard layers

Standard layer depth/m	
depth≤100 m	100 m<depth≤200 m
0	0
10	10
20	30
30	50
40	75
50	100
75	150
100	200

Table 2. HPLC mobile phase gradient table

Time/min	Mobile phase A/%	Mobile phase B/%
0	75	25
1	50	50
15	0	100
25	0	100
26	75	25
36	75	25

Table 3. Pigments measured by HPLC experiments

Pigment name	Short name
Chlorophyll *a*	Chl *a*
Divinyl chlorophyll *a*	DV Chl *a*
Divinyl chlorophyll *b*	DV Chl *b*
Chlorophyll *b*	Chl *b*
Chlorophyll c_2	Chl c_2
Chlorophyll c_3	Chl c_3
Peridinin	Perid
Fucoxanthin	Fuco
Diadinoxanthin	Diad
Alloxanthin	Allo
Violaxanthin	Viol
β-carotene	Beta
19′-butanoyloxy-fucoxanthin	19′-But
19′-hexanoyloxy-fucoxanthin	19′-Hex
Zeaxanthin	Zea

In this study, we chose five main species of the phytoplankton community for analysis and calculated each contribution based on diagnostic pigments (Hirata et al., 2011), they were diatoms, dinoflagellates, green algae, prokaryotes and prochlorococcus, respectively. Accordingly, the five diagnostic pigments, Fuco, Perid, Chl *b*, Zea and DV Chl *a*, were selected.

3 Results

3.1 *Remote sensing hydrology and Chl a*

The East Asian monsoon was set up in the NSCS with southern wind prevailing along the EHC and ELPC since May 2015 when it begun to trigger the EHU and ELPU and drive offshore cold SST tongue with negative SLA and surface high Chl *a* (Fig. 2). It can be seen that the EHU appeared along the EHC within 50 m isobaths from the Lingshui coast to the Qizhou Archipelagoes and contained two upwelling centers in which one showed up at the Qionghai coast (19.2°N, 110.6°E) due to wind-enforced offshore Ekman pumping (Xie et al., 2012) and another showed up at the Qizhou Archipelagoes (20°N, 111.2°E) due to interaction between abrupt topography and coastal current (Su and Pohlmann, 2009; Jing et al., 2015). The EHU was enhanced to peak driven by augmented upwelling-favorable southwestern wind from June to July when inshore SST was about 2.0°C lower than the offshore water. It was reduced to almost disappearance from August to September when wind was weakened and shifted from southwestward to southeastward (Fig. 2). In response to outbreak of the upwelling, the surface high Chl *a* band occupied the EHC with about 0.5–1.5 mg/m^3 concentration at the upwelling center during May. It extended farthest over 50 m isobaths during July and retreated within 50-m isobaths again but remained high values (about 0.5–1.0 mg/m^3) from August to September at the EHU.

The monthly variation of the ELPU has similar trend with the EHU during the period. It centered at (20.4°N, 111°E) with relative weaker upwelling due to its wide and gentle slope of topography but with much higher surface Chl *a* concentration eutrophicated by plentiful coastal nutrient input from the ELPC compared with the EHU (Zeng et al., 2015; Feng et al., 2019). The Chl *a* concentration generally reached about 2.0–4.0 mg/m^3 at the ELPU. The ELPU was still significant with extremely high surface Chl *a* existing within 50 m isobaths along ELPC in September because of increase of SST and rich nutrient input from coast (Feng et al., 2019).

Figure 3 shows the averaged SST, SLA and surface Chl *a* concentration at the EHU and ELPU during the cruise period from 29 July to 7 August in 2015 based on satellite remote sensing daily dataset. Noted that although the EHU and ELPU was weakened largely during the period, surface phytoplankton was still blooming at the upwelling areas and extending over 50 m isobaths. Given that, the cruise was taken in the right time to measure and represent phytoplankton community at the EHU and ELPU during the upwelling season.

3.2 *Survey hydrology*

The hydrologic structures of the EHU and ELPU have been illustrated by many previous surveys in which lower temperature and higher salinity water were pumped from deep layer to surface (Su and Pohlmann, 2009; Jing et al., 2009, 2011, 2015). Our survey results have similar hydrologic structures with previous studies during the upwelling season. The horizontal distributions at different layers from surface (4 m) to 50 m and transection vertical profiles at five representative transections of temperature, salinity and DO at the EHU and ELPU were plotted in Figs 4 and 5, respectively. In accordance with satellite SST images, the surface low-temperature and high-salinity belt stretched from Lingshui to the ELPC and three upwelling centers showed up in which the surface water was 2.0–3.0°C colder and 0.5 psu saltier than offshore water (Fig. 4). Driven by the upwelling, the isotherms and isohalines were squeezed to build a strong thermohaline front and uplifted to ventilate air at the EHU. It can be seen that 24°C isotherm and 34.3 psu isohaline were ventilated from about 60 m depth layer to surface. At subsurface 10-m layer the belt was extended to near 25 km offshore and the temperature and salinity gradients were augmented, which was comparable with other observation (Jing et al., 2009). The belt was extended further to near 100 m isobaths and over 40 km offshore at the 50 m layer. At 100 m depth, the thermohaline isolines became almost even and upwelling was much weakened (Fig. 5). The ELPU was relative weaker than the EHU due to the gentle slope and strong stratification in which 26°C isotherm and 34.1 psu isohaline were ventilated from about 10 m depth layer.

3.3 *Survey DO*

At the EHU, DO distributions showed different pattern at dif-

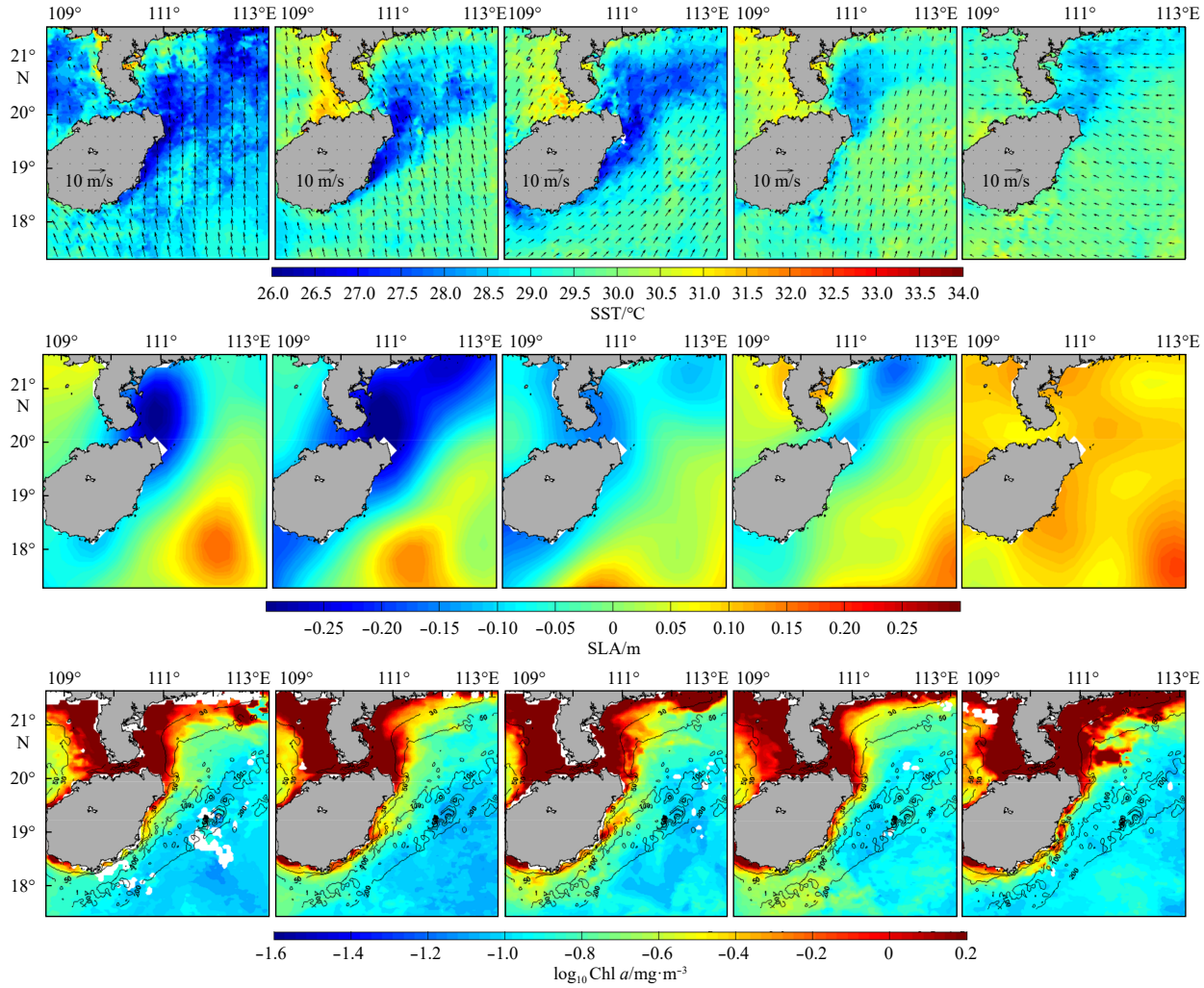

Fig. 2. The distributions of monthly averaged remote sensing SST with wind field (upper panel), sea level anomaly (middle panel) and chlorophyll *a* (lower panel) at the EHC from May to September of 2015.

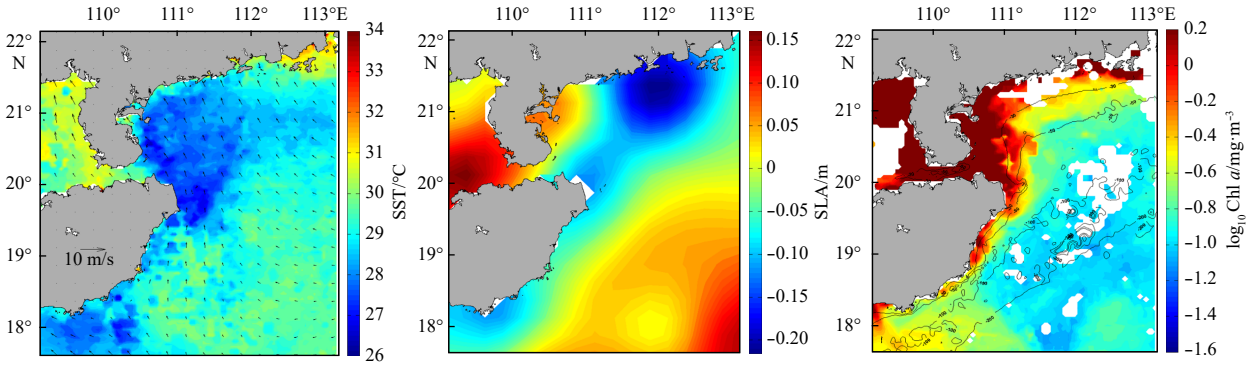

Fig. 3. The distributions of averaged remote sensing SST with wind field, sea level anomaly and chlorophyll *a* at the EHC during the cruise.

ferent layers. The surface DO were generally 1.0 mg/L higher than offshore water and maximum value reached about 8.0 mg/L near the Qionghai coast. Vertical profiles in Fig. 5 show that the high values can extend downward to 20 m depth owing to river discharge input (Wang et al., 2015). Contrarily, bottom anoxia water with values less than 6 mg/L were carried upward along the slope under 30 m depth by the wind-driven upwelling indicating 30 m depth as an interface to distinguish the impacts of the two dynamic processes on biochemical characteristics at the EHU. The values of DO at the ELPU were relative lower than that at the EHU due to large amount of COD and BOD in this area (Feng et al., 2019). In overall, surface DO at the ELPU were about 1.0 mg/L lower than surrounding surface water and its minimum value reached about 5.0 mg/L. Beneath the surface, the DO were con-

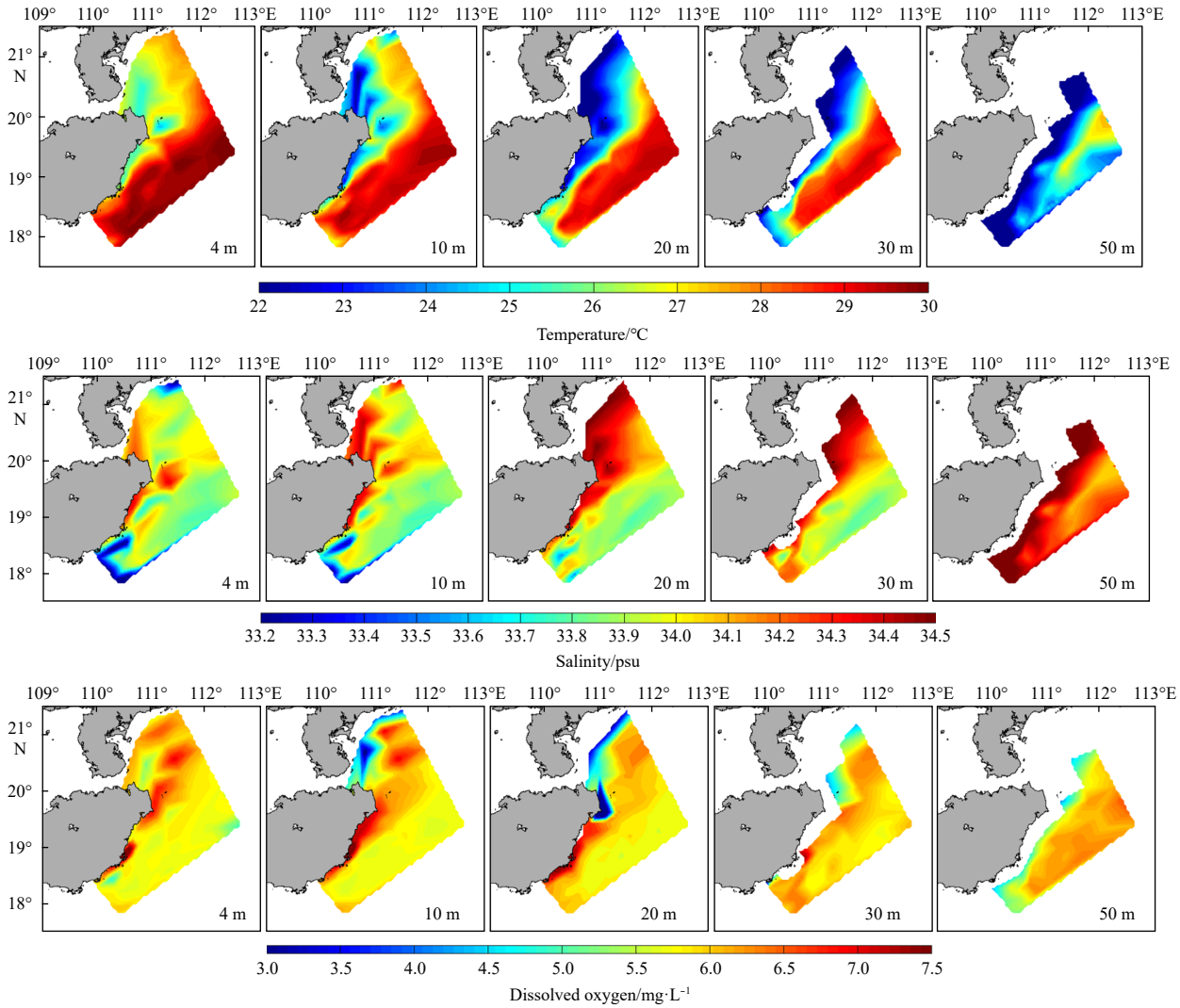

Fig. 4. The distributions of observed temperature (upper panel), salinity (middle panel) and DO (lower panel) at 4 m, 10 m, 20 m, 30 m and 50 m depth layers at the EHC during the cruise.

sumed largely that led a severe anoxia condition at the ELPU, especially at the bottom area with <3.5 mg/L DO concentration.

3.4 *Total Chl a*

We summarized all amounts of the phytoplankton species based on 15 pigment analysis and obtained the total Chl *a* in the upwelling area at different standard depth levels (Fig. 6). Similar with remote sensing Chl *a* pattern, it can be seen that surface total Chl *a* concentrations of the inshore water showed much higher values than that of the offshore water (0.2–0.3 mg/m^3) due to rich nutrient supply from coasts (Zeng et al., 2015, Feng et al., 2019). The maximum values can reach 1.0 mg/m^3 and 4.0 mg/m^3 at the EHU and ELPU, respectively, which were comparable with remote sensing results (Fig. 3) and previous surveys (Chen et al., 2016; Feng et al., 2019). And this distinct differences of phytoplankton biomass between inshore and offshore was constant with trend in the NSCS (Chen et al., 2006; Zhai et al., 2011). At subsurface layer of 10 m, maximum total Chl *a* was reduced to 0.5 mg/m^3 at the Qionghai coast, while phytoplankton biomass bloomed extensively at 30 m layer in which maximum total Chl *a* reached about 1.5 mg/m^3. And the blooming of phytoplankton biomass at middle layer of this upwelling area also was found by Chen et al. (2016). The thermohaline images in Fig. 5 show that bottom water only can be pumped up to 30–40 m depth layer at this area which helped to block upward supply of nutrient to subsurface but nourish phytoplankton underneath. At the Qizhou Archipelagoes, phytoplankton biomass grew up to over 1.5 mg/m^3 at the subsurface of 10 m depth where bottom rich-nutrient water were easily to be pumped up to this layer. The phytoplankton biomass at the ELPU was decreased gradually with water depth likely due to photosynthesis reduction by shade of surface blooming algae. To the deeper area, total Chl *a* concentration were reduced largely at the upwelling areas but still somewhat higher than offshore water at 50 m layer (Fig. 6) and it became same level as the open sea in the NSCS at 100 m layer (not shown).

3.5 *Phytoplankton community*

Phytoplankton community structure usually vary with different marine bio-physical systems under impacts of coastal upwelling (Li et al., 2014), mesoscale eddy (Huang et al., 2010), river plume front (Li et al., 2018) and typhoon (Tsuchiya et al., 2013, Xie et al., 2017) etc. Among them, upwelling is most ubiquitous

dynamic process to take nutrient underlying to upper layer and change phytoplankton community in coastal area (Eppley and Thomas, 1969). Basically, phytoplankton can be divided into three types according to the particle size, microplankton (>20 μm), nanoplankton (2–20 μm) and picoplankton (0.2–2 μm) in which diatom (micro), dinoflagellates (micro), green algae (nano) abundances are the most representative marine biomarkers (Sieburth et al., 1978). In addition, we found other two picoplank-

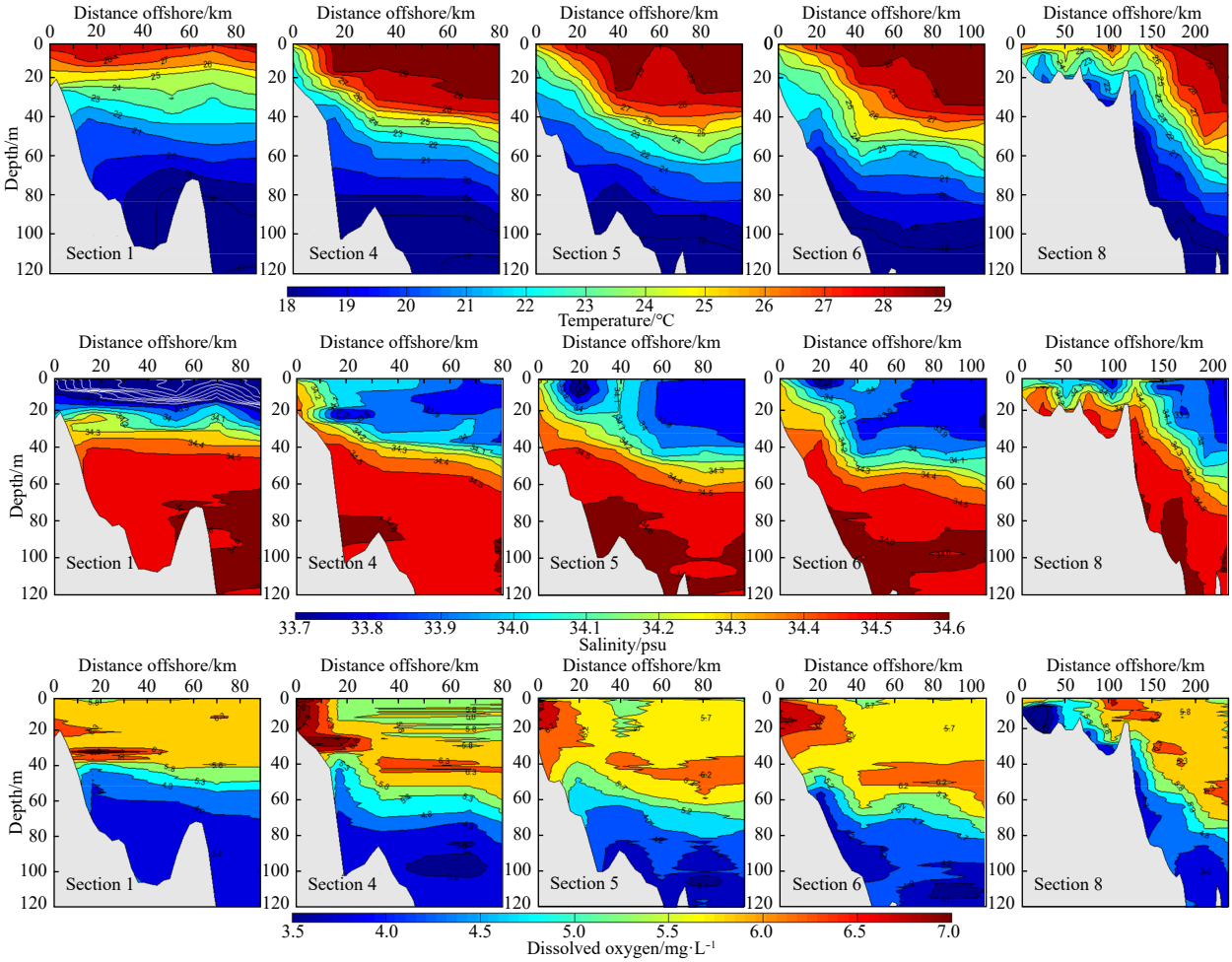

Fig. 5. The vertical distributions of observed temperature (upper panel), salinity (middle panel) and DO (lower panel) along S1, S4, S5, S6 and S8 transections during the cruise.

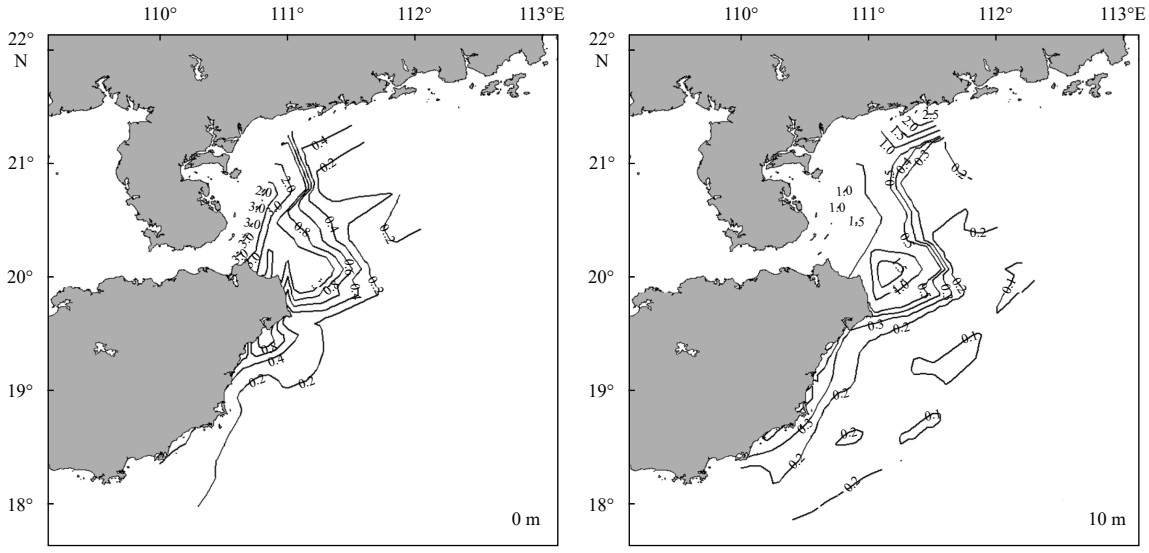

Fig. 6.

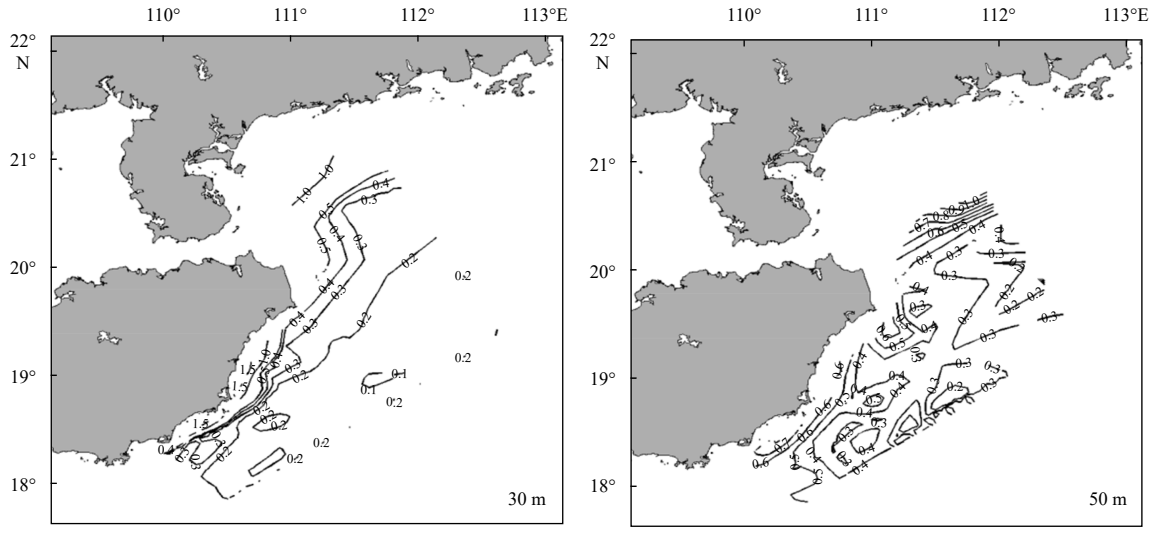

Fig. 6. Total Chl *a* distributions (mg/m^3) at surface, 10 m, 30 m and 50 m depth layers at the EHC during the cruise.

ton abundances, prokaryotes and prochlorococcus, were nonignorable besides the three main types of phytoplankton, especially at the offshore area. For comparison, contributions of five phytoplankton groups to total Chl *a* were calculated and expressed as Chl *a* concentration (mg/m^3) based on diagnostic pigment analysis at the EHU and ELPU.

As we know, diatom is more prevalent in eutrophic waters and its growth ability is high even at low temperature with high nutrition levels (Peng et al., 2006; Hirata et al., 2011). Indeed, the phytoplankton categorization in our study show that diatom were the main population which account up to 50% phytoplankton abundances at the inshore of the EHU (Figs 7 and 8). Its abundance was decreased to 10% with increasing depth and distance from inshore gradually and replaced by prokaryotes (about 50%), green algae (about 20%) and prochlorococcus (20%) at the continental shelf area. The dinoflagellates has least contribution to phytoplankton community at the EHU. Zeng et al. (2015) stated that nutrient concentration were relatively low and nitrogen- and silica-limitation prevailed at the EHU. While, diatom is sensitive to silica-limitation and prokaryotes is more suitable for growing in oligotrophic area (Hallegraeff, 1981; Tilman et al., 1986; Örnólfsdóttir et al., 2004). Different with the EHU, nutrient concentration were relative high and phosphorus-limitation was prevailing in the ELPU during summer and fall (Feng et al., 2019). As a result, diatom dominated phytoplankton population and it can account up to 80% of phytoplankton abundances in this upwelling area. Green algae (about 10%) was secondary to diatom and prochlorococcus (about 5%) for the next. And prokaryotes and dinoflagellates contributed very small portion for phytoplankton biomass. At the offshore of the ELPU, phytoplankton structure was similar with the offshore of the EHU in which prokaryotes and prochlorococcus abundances were relative high from surface to 30 m, while green algae abundance rose up under 30 m.

4 Discussion

4.1 *Physical control on DO and Chl a distributions*

The importance of upwelling on controlling surface phytoplankton bloom at the EHU were recognized extensively (Deng et al., 1995; Jing et al., 2011; Xie et al., 2012). However, we found the peak value of Chl *a* concentration occurring at 30 m depth rather than surface at the upwelling center of the EHU (Fig. 6). In addition, DO distribution also showed high value at this layer (lower panel in Fig. 5). The themerhaline structures revealed that this kind of sandwich structures of DO and Chl *a* were controlled by physical dynamics. The upwelling-favorable summer monsoon driven offshore Ekman drift at the Qionghai coast that carried cold and salt bottom water with low DO to upper mixing layer and suppressed warm and fresh water with high DO to thermohaline layer. Together with bottom cold and saltier water with low DO, such a sandwich structure of DO was formed. The high value of DO at the nearshore of the Qionghai may was originated from the freshwater discharge from coast rivers (Wang et al., 2015). It can be seen that strong vertical stratification was built at 30–40 m depth under thermohaline layer that may restored nutrient and conduced to phytoplankton growth at this layer. However, the relative rich nutrient water upwelled from bottom may be diluted by oligotrophic water at surface to subsurface layers that was unfavorable of phytoplankton growth at these layers.

4.2 *Phytoplankton species*

At the EHU, the dominant phytoplankton specie was diatom during the survey since diatom can bloom more prevalently than other speices in eutrophic water with low temperature (Peng et al., 2006; Hirata et al., 2011). It was often observed at upwelling systems over the world such as the northwestern and western Gulf of Mexico, the Algarrobo Bay in Chile, the southern Benguela, the northeastern Black Sea, the western Taiwan Strait, and the southeast coast of Algarve (Lambert et al., 1999; Wang et al., 2016; Anglès et al., 2019; Sañé et al., 2019; Silkin et al., 2019; Ferreira et al., 2020; Burger et al., 2020). However, unlike some other upwelling systems, our results showed that green algae and prokaryotes were the second dominant species at the EHU while dinoflagellate has least contribution to phytoplankton community. Neverthless, dinoflagellate takes second place at the western Taiwan Strait, northwestern Gulf of Mexico, and the Algarve coast (Wang et al., 2016; Anglès et al., 2019; Sañé et al., 2019). We summarized the potential reasons for the difference of species among different ecosystems: (1) the intensity of the upwelling varies from each other and the phytoplankton community show different response to the nutrition concentration in-

fluenced by the upwelling intensity (Li et al., 2014); (2) the thermohaline structure was different and stratification was relative strong in the EHU. It impeded upward transport of the nutrient and caused unfavorable conditions for some phytoplankton species growth at the upper layers, while some species are more suitable for growing in the oligotrophic area (Hallegraeff, 1981; Tilman et al., 1986; Örnólfsdóttir et al., 2004).

4.3 *Relation with climate event*

Jing et al. (2011) analyzed long-term remote sensing data during 1997–2007 and found the relation between upwelling intensity of the EHU and El Niño index. They reported that the enhanced wind stress curl during El Niño year can drive stronger upwelling of the EHU and induce larger amount of phytoplankton biomass than other normal years. Xie et al. (2016) gave the

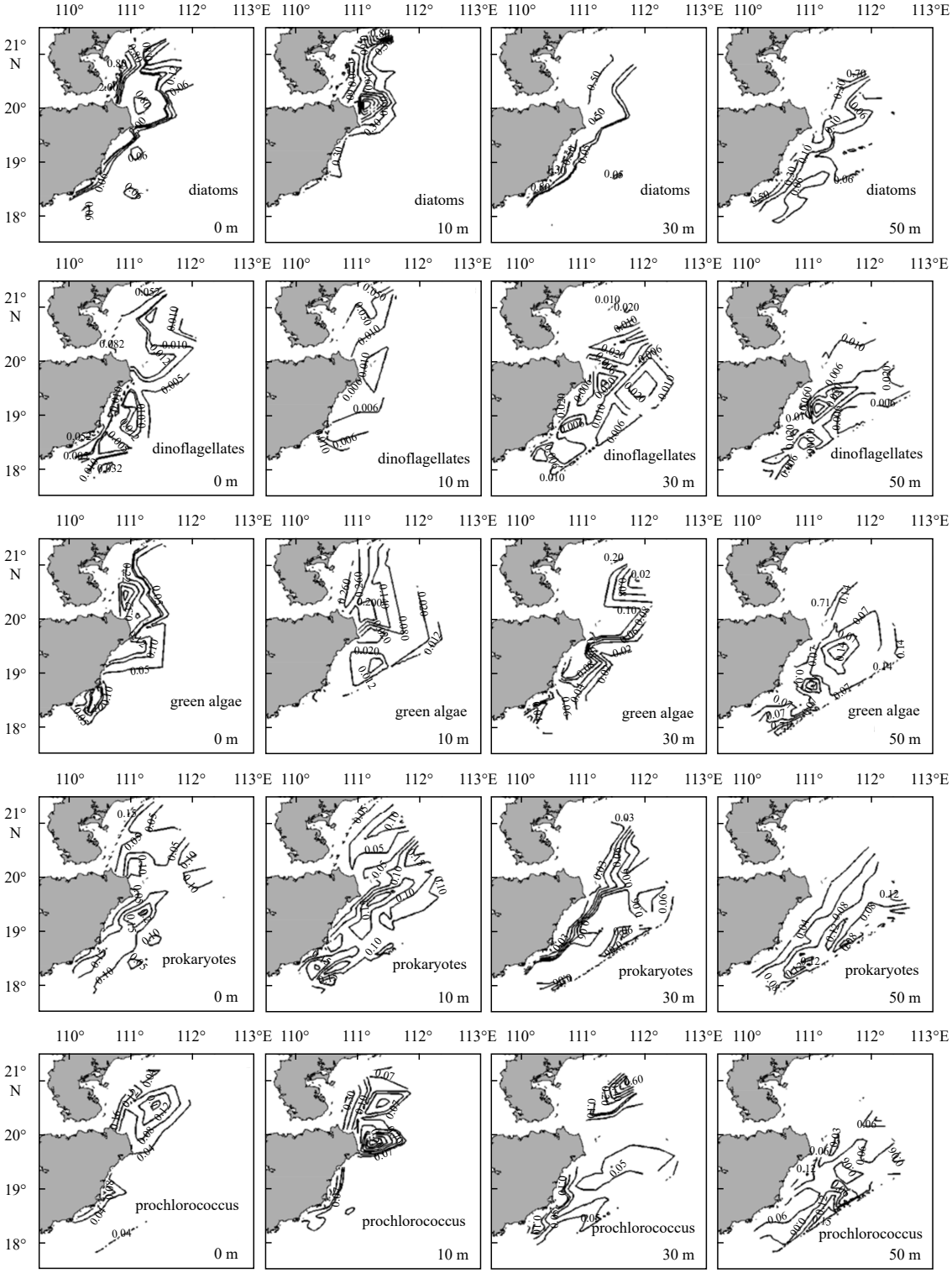

Fig. 7. The abundance distributions (expressed as Chl *a* concentration) of five phytoplankton species to total Chl *a* (mg/m^3) at surface, 10 m, 30 m, and 50 m depth layer during the cruise.

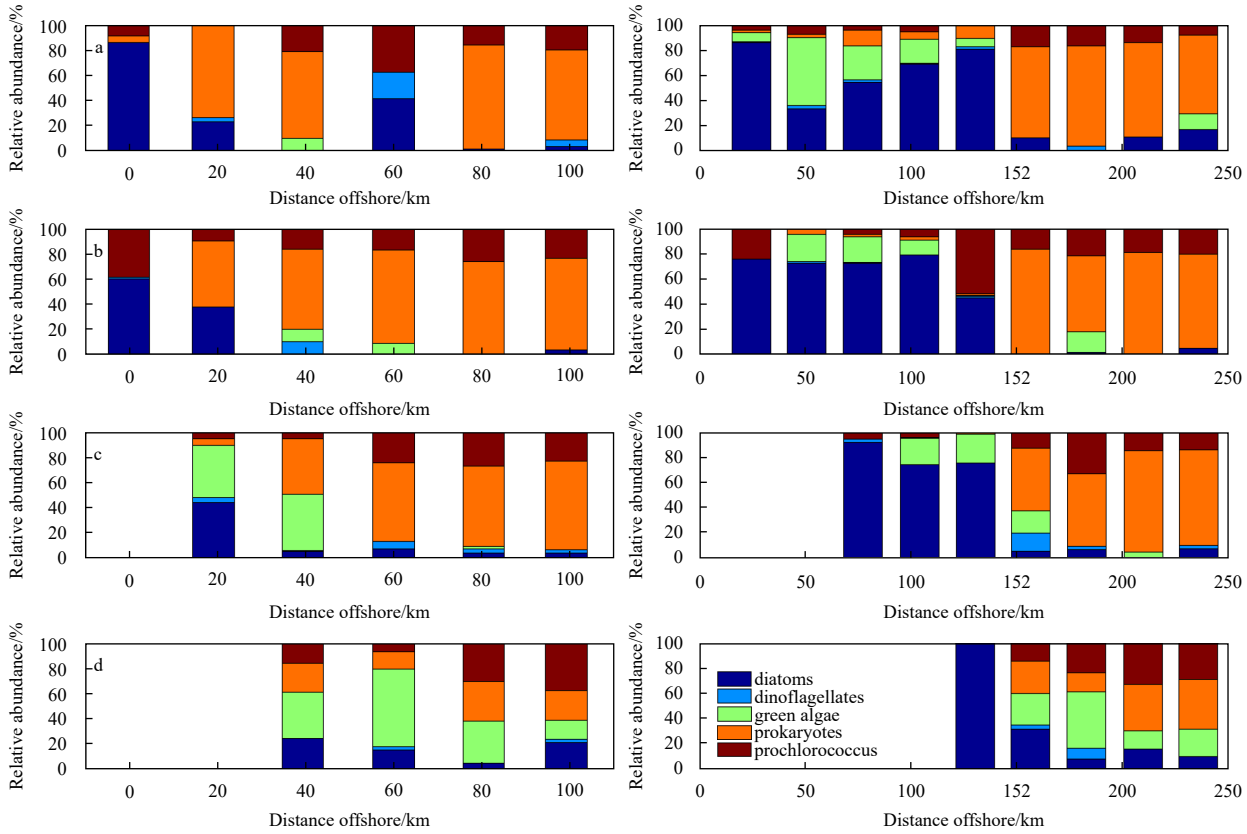

Fig. 8. The relative abundance of five phytoplankton species (%) at representative transections S5 for the EHU (left panel) and S8 for the ELPU (right panel) at surface (a), 10 m (b), 30 m (c) and 50 m (d) depth layers during the cruise.

similar conclusion of upwelling trend based on longer reanalysis dataset during 1982–2012. And this trend of upwelling variation modulated by climate event can be recorded by coastal coral at this area (Liu et al., 2009). The year of 2015, as we know, was a relative strong El Niño year (Xue and Kumar, 2017). And the Niño 3.4 index presented a significant positive SST signal and wind stress at the EHU was strengthened accordingly during summer 2015 (Fig. 9). To examine the differences of phytoplankton biomass between 2015 and other years, we calculated the Chl *a* concentration at the EHU using recent remote sensing dataset during 2000–2018. Different with Jing et al. (2011), our results illustrated that the Chl *a* during summer 2015 was leading other normal years indistinctively and even less in some case (Fig. 9). To prove that, we compared two survey results between our and previous cruises at the EHU. Zeng et al. (2015) measured the surface Chl *a* concentration at the EHU during summer 2013 as a normal year and its maximum value (about 2.0 mg/m^3, see Fig. 2 in their paper) exceeded our survey result in this study at the Qionghai coast. It can be understood that the phytoplankton dynamics is a very complex process and can be impacted by many factors besides physical process, such as nutrient condition, pH value etc. To further diagnose the relation between the phytoplankton biomass variations at the EHU and large-scale climate event, more processes will need to be considered in future work.

5 Conclusions

In this study, we analyzed multiple remote sensing datasets and survey data to explore the physical structure, DO distribution, phytoplankton biomass and community during summer 2015 at the EHU and its adjacent upwelling area, the ELPU. There was a significant cold band with three upwelling centers of high salinity and low temperature at the EHU and ELPU driven by upwelling-favorable summer monsoon in which they were located at the Qionghai coast, the Qizhou Archipelagoes and the ELPC. And the inshore water was 2.0–3.0°C colder and 0.5 psu saltier than offshore water at surface at the upwelling system generally. The EHU was significantly stronger than the ELPU where 24°C isotherm and 34.3 psu isohaline can ventilate from about 60 m depth layer to surface. Base on survey results, we found water environmental condition at the EHU was healthier than the ELPU. At the upper layer of the EHU, DO values were larger than 6.0 mg/L from surface to 30 m depth. Beneath this depth, DO values were ranged from 4.0 mg/L to 6.0 mg/L generally. While, DO values at the ELPU were less than 6.0 mg/L in whole water column, especially at the bottom layer where its values were less than 3.5 mg/L owing to abundant COD and BOD. There was significant augment of the phytoplankton biomass at middle layer of 30 m at the EHU in which rich-nutrient water were pumped to this layer. The phytoplankton biomass at the ELPU were much higher than the EHU where the maximal value can reach about 4.0 mg/m^3 due to its plentiful nutrient input. Form the inshore to offshore, five species of phytoplankton community dominated the EHU and ELPU. At the inshore of the EHU, the phytoplankton community was dominated by diatom which accounted for about 50% of phytoplankton biomass. Nevertheless, prokaryotes (about 40%), green algae (about 20%) and prochlorococcus (about 20%) dominated the offshore of the EHU. At the ELPU, diatom accounted for about 80% of phytoplankton biomass and green algae was secondary to it. Compared with previous survey, we found there was no significant increase of phytoplankton biomass in this El

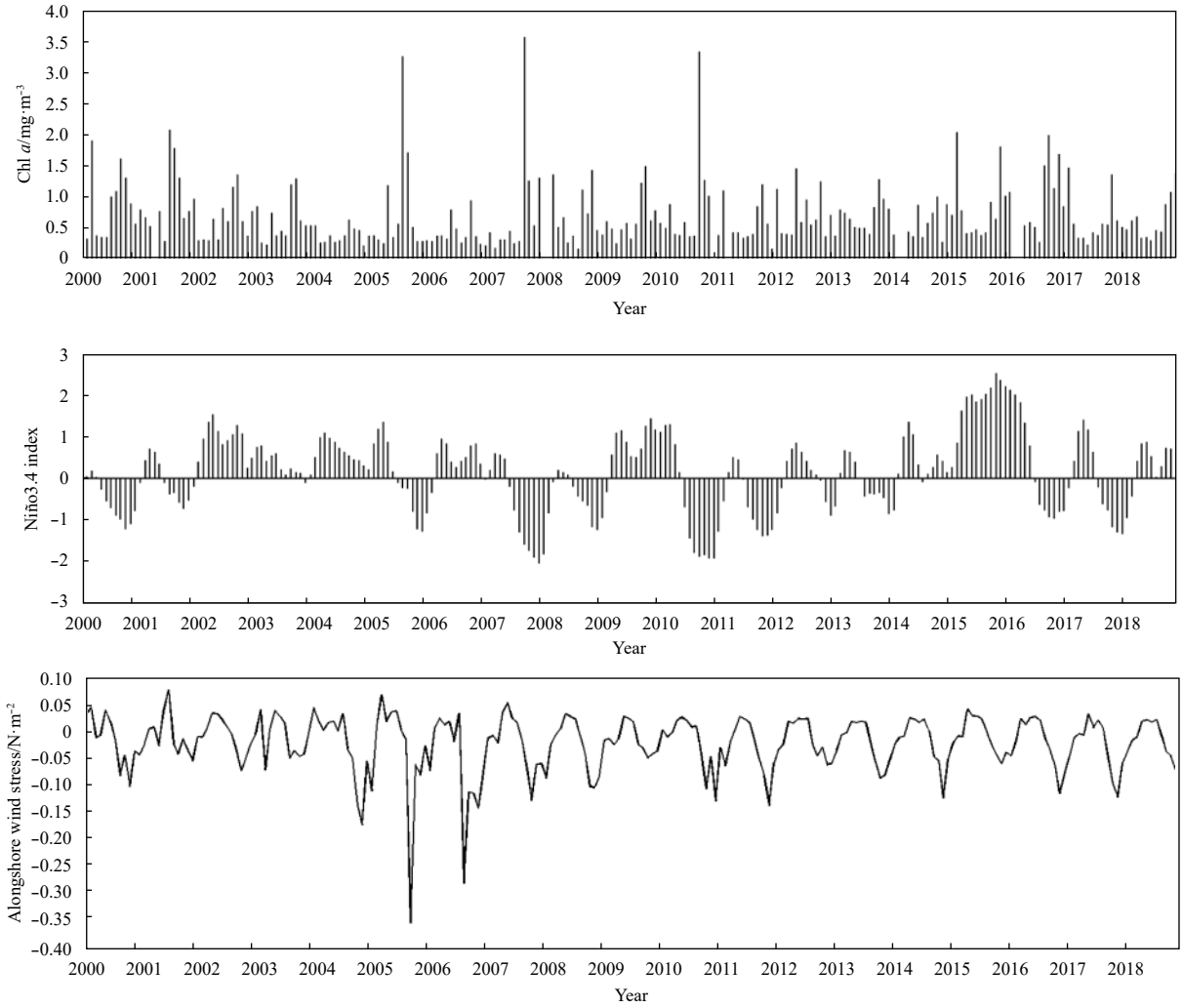

Fig. 9. Monthly variation of Chl *a* at the EHU (upper panel), Niño 3.4 index (middle panel) and alongshore wind stress (lower panel) during 2000–2018.

Niño year and more studies need to be conducted to investigate the relation between phytoplankton distribution and climate event.

References

Anglès S, Jordi A, Henrichs D W, et al. 2019. Influence of coastal upwelling and river discharge on the phytoplankton community composition in the northwestern Gulf of Mexico. Progress in Oceanography, 173: 26–36, doi: 10.1016/j.pocean.2019.02.001

Benson S R, Croll D A, Marinovic B B, et al. 2002. Changes in the cetacean assemblage of a coastal upwelling ecosystem during El Niño 1997–98 and La Niña 1999. Progress in Oceanography, 54(1–4): 279–291, doi: 10.1016/S0079-6611(02)00054-X

Burger J M, Moloney C L, Walker D R, et al. 2020. Drivers of short-term variability in phytoplankton production in an embayment of the southern Benguela upwelling system. Journal of Marine Systems, 208: 103341, doi: 10.1016/j.jmarsys.2020.103341

Chen Fajin, Zeng Zhen, Meng Yafei, et al. 2016. Diel variation of nutrients and chlorophyll *a* concentration in the Qiongdong sea region during the summer of 2013. Haiyang Xuebao (in Chinese), 38(4): 76–83

Chen Jixin, Huang Bangqin, Liu Yuan, et al. 2006. Phytoplankton community structure in the transects across East China Sea and northern South China Sea determined by analysis of HPLC photosynthetic pigment signatures. Advances in Earth Science, 21(7): 738–746

Deng Song, Zhong Huangliang, Wang Mingwen, et al. 1995. On relation between upwelling off Qionghai and fishery. Journal of Oceanography in Taiwan Strait (in Chinese), 14(1): 51–56

Du Xiuning, Peterson W T. 2018. Phytoplankton community structure in 2011–2013 compared to the extratropical warming event of 2014–2015. Geophysical Research Letters, 45(3): 1534–1540, doi: 10.1002/2017GL076199

Emeis K, Eggert A, Flohr A, et al. 2018. Biogeochemical processes and turnover rates in the northern Benguela upwelling system. Journal of Marine Systems, 188: 63–80, doi: 10.1016/j.jmarsys.2017.10.001

Eppley R W, Thomas W H. 1969. Comparison of half-saturation constants for growth and nitrate uptake of marine phytoplankton. Journal of Phycology, 5(4): 375–379, doi: 10.1111/j.1529-8817.1969.tb02628.x

Feng Yuting, Zhao Hui, Shi Yuzhen. 2019. The concentration of nutrients and chlorophyll a in the offshore of Leizhou Peninsula in autumn spatial distribution and their relationship. Journal of Guangdong Ocean University (in Chinese), 39(2): 75–82

Ferreira A, Sa C, Silva N, et al. 2020. Phytoplankton response to nutrient pulses in an upwelling system assessed through a microcosm experiment (Algarrobo Bay, Chile). Ocean and Coastal Management, 190: 105167, doi: 10.1016/j.ocecoaman.2020.105167

Gan Jianping, Cheung A, Guo Xiaogang, et al. 2009. Intensified up-

welling over a widened shelf in the northeastern South China Sea. Journal of Geophysical Research: Oceans, 114(C9): C09019, doi: 10.1029/2007JC004660

Guo Fei, Shi Maochong, Xia Zongwan. 1998. Two-demension diagnose model to calculate upwelling on offshore of the east coast of Hainan Island. Haiyang Xuebao (in Chinese), 20(6): 109–116

Hallegraeff G M. 1981. Seasonal study of phytoplankton pigments and species at a coastal station off Sydney: Importance of diatoms and the nanoplankton. Marine Biology, 61(2–3): 107–118, doi: 10.1007/BF00386650

Han Wuying, Wang Mingbiao, Ma Kemei. 1990. On the lowest surface water temperature area of China Sea in summer-the upwelling along the east coast of Hainan island. Oceanologia et Limnologia Sinica (in Chinese), 21(3): 267–275

Hirata T, Hardman-mountford N J, Brewin R J W, et al. 2011. Synoptic relationships between surface chlorophyll-*a* and diagnostic pigments specific to phytoplankton functional types. Biogeosciences, 8(2): 311–327, doi: 10.5194/bg-8-311-2011

Hong Qiming, Li Li. 1991. A study of upwelling over continental shelf off eastern Guangdong. Journal of Oceanography in Taiwan Strait (in Chinese), 10(3): 271–277

Huang Bangqin, Hu Jun, Xu Hongzhou, et al. 2010. Phytoplankton community at warm eddies in the northern South China Sea in winter 2003/2004. Deep Sea Research Part II: Topical Studies in Oceanography, 57(19–20): 1792–1798, doi: 10.1016/j.dsr2.2010.04.005

Jing Zhiyou, Qi Yiquan, Du Yan. 2011. Upwelling in the continental shelf of northern South China Sea associated with 1997–98 El Niño. Journal of Geophysical Research: Oceans, 116(C2): C02033, doi: 10.1029/2010JC006598

Jing Zhiyou, Qi Yiquan, Du Yan, et al. 2015. Summer upwelling and thermal fronts in the northwestern South China Sea: Observational analysis of two mesoscale mapping surveys. Journal of Geophysical Research: Oceans, 120(3): 1993–2006, doi: 10.1002/2014JC010601

Jing Zhiyou, Qi Yiquan, Hua Zulin, et al. 2009. Numerical study on the summer upwelling system in the northern continental shelf of the South China Sea. Continental Shelf Research, 29(2): 467–478, doi: 10.1016/j.csr.2008.11.008

Lü Xingang, Qiao Fangli, Wang Guansuo, et al. 2008. Upwelling off the west coast of Hainan Island in summer: Its detection and mechanisms. Geophysical Research Letters, 35(2): L02604, doi: 10.1029/2007GL032440

Lü Xingang, Qiao Fangli, Xia Changshui, et al. 2010. Upwelling and surface cold patches in the Yellow Sea in summer: Effects of tidal mixing on the vertical circulation. Continental Shelf Research, 30(6): 620–632, doi: 10.1016/j.csr.2009.09.002

Lambert C D, Bianchi T S, Santschi P H. 1999. Cross-shelf changes in phytoplankton community composition in the Gulf of Mexico (Texas shelf/slope): The use of plant pigments as biomarkers. Continental Shelf Research, 19(1): 1–21, doi: 10.1016/S0278-4343(98)00075-2

Lehmann A, Myrberg K. 2008. Upwelling in the Baltic Sea—A review. Journal of Marine Systems, 74(S1): S3–S12

Li Li. 1993. Summer upwelling system over the northern continental shelf of the South China Sea—Physical description. In: Su J, Chuang W S, Hsurh R Y, eds. Proceedings of the Symposium on the Physical and Chemical Oceanography of the China Seas. Beijing: China Ocean Press, 58–68

Li Li, Liu Jie, He Juan, et al. 2014. Factors affecting the abundance and community structure of the phytoplankton in northern South China Sea in the summer of 2008: A biomarker study. Chinese Science Bulletin, 59(10): 981–991, doi: 10.1007/s11434-013-0106-4

Li Yineng, Peng Shiqiu, Yang Wei, et al. 2012. Numerical simulation of the structure and variation of upwelling off the east coast of Hainan Island using QuikSCAT winds. Chinese Journal of Oceanology and Limnology, 30(6): 1068–1081, doi: 10.1007/s00343-012-1275-8

Li Kaizhi, Yin Jianqiang, Huang Liangmin, et al. 2010. Monsoon-forced distribution and assemblages of appendicularians in the northwestern coastal waters of South China Sea. Estuarine, Coastal and Shelf Science, 89(2): 145–153, doi: 10.1016/j.ecss.2010.06.001

Li Kaizhi, Yin Jianqiang, Huang Liangmin, et al. 2011. Distribution and abundance of thaliaceans in the northwest continental shelf of South China Sea, with response to environmental factors driven by monsoon. Continental Shelf Research, 31(9): 979–989, doi: 10.1016/j.csr.2011.03.004

Li Q P, Zhou Weiwen, Chen Yinchao, et al. 2018. Phytoplankton response to a plume front in the northern South China Sea. Biogeosciences, 15(8): 2551–2563, doi: 10.5194/bg-15-2551-2018

Lin Peigen, Hu Jianyu, Zheng Quanan, et al. 2016. Observation of summertime upwelling off the eastern and northeastern coasts of Hainan Island, China. Ocean Dynamics, 66(3): 387–399, doi: 10.1007/s10236-016-0934-2

Liu Yi, Peng Zicheng, Wei Gangjian, et al. 2009. Variation of summer coastal upwelling at northern South China Sea during the last 100 years. Geochimica (in Chinese), 38(4): 317–322

Örnólfsdóttir E B, Lumsden S E, Pinckney J L. 2004. Phytoplankton community growth-rate response to nutrient pulses in a shallow turbid estuary, Galveston Bay, Texas. Journal of Plankton Research, 26(3): 325–339, doi: 10.1093/plankt/fbh035

Pauly D, Christensen V. 1995. Primary production required to sustain global fisheries. Nature, 374(6519): 255–257, doi: 10.1038/374255a0

Peng Xin, Ning Xiuren, Cai Yiming, et al. 2006. Review of research on the bottom-up effects of phytoplankton growth. Journal of Marine Sciences (in Chinese), 24(3): 64–75

Roy C, Reason C. 2001. ENSO related modulation of coastal upwelling in the eastern Atlantic. Progress in Oceanography, 49(1–4): 245–255, doi: 10.1016/S0079-6611(01)00025-8

Sañé E, Valente A, Fatela F, et al. 2019. Assessment of sedimentary pigments and phytoplankton determined by CHEMTAX analysis as biomarkers of unusual upwelling conditions in summer 2014 off the SE coast of Algarve. Journal of Sea Research, 146: 33–45, doi: 10.1016/j.seares.2019.01.007

Shu Yeqiang, Wang Dongxiao, Feng Ming, et al. 2018. The contribution of local wind and ocean circulation to the interannual variability in coastal upwelling intensity in the northern South China Sea. Journal of Geophysical Research: Oceans, 123(9): 6766–6778, doi: 10.1029/2018JC014223

Sieburth J M, Smetacek V, Lenz J. 1978. Pelagic ecosystem structure: Heterotrophic compartments of the plankton and their relationship to plankton size fractions. Limnology and Oceanography, 23(6): 1256–1263, doi: 10.4319/lo.1978.23.6.1256

Silkin V A, Pautova L A, Giordano M, et al. 2019. Drivers of phytoplankton blooms in the northeastern Black Sea. Marine Pollution Bulletin, 138: 274–284, doi: 10.1016/j.marpolbul.2018.11.042

Smith R L. 1995. The physical processes of coastal ocean upwelling systems. In: Summerhayes C P, Emeis K C, Angel M V, et al, eds. Upwelling in the Ocean: Modern Processes and Ancient Records. Chichester: John Wiley and Sons, 18: 39–64

Sobarzo M, Bravo L, Donoso D, et al. 2007. Coastal upwelling and seasonal cycles that influence the water column over the continental shelf off central Chile. Progress in Oceanography, 75(3): 363–382, doi: 10.1016/j.pocean.2007.08.022

Su Jian, Pohlmann T. 2009. Wind and topography influence on an upwelling system at the eastern Hainan coast. Journal of Geophysical Research: Oceans, 114(C6): C06017, doi: 10.1029/2008JC005018

Su Jian, Wang Jun, Pohlmann T, et al. 2011. The influence of meteorological variation on the upwelling system off eastern Hainan during summer 2007–2008. Ocean Dynamics, 61(6): 717–730, doi: 10.1007/s10236-011-0404-9

Su Jian, Xu Mingquan, Pohlmann T, et al. 2013. A western boundary upwelling system response to recent climate variation (1960–2006). Continental Shelf Research, 57: 3–9, doi: 10.1016/j.csr.2012.05.010

Tilman D, Kiesling R, Sterner R, et al. 1986. Green, blue-green and di-

atom algae: taxonomic differences in competitive ability for phosphorus, silicon and nitrogen. Archiv Fur Hydrobiologie, 106(4): 473–485

Tsuchiya K, Kuwahara V S, Yoshiki T M, et al. 2013. Phytoplankton community response and succession in relation to typhoon passages in the coastal waters of Japan. Journal of Plankton Research, 36(2): 424–438

van Heukelem L, Thomas C S. 2001. Computer-assisted high-performance liquid chromatography method development with applications to the isolation and analysis of phytoplankton pigments. Journal of Chromatography A, 910(1): 31–49, doi: 10.1016/S0378-4347(00)00603-4

Wang Mengyin, Hu Qiwei. 2017. Impact of summer upwelling on the fisheries resources in the northern South China Sea based on remote sensing data. Journal of Hainan Tropical Ocean University (in Chinese), 24(2): 22–29

Wang Yu, Kang Jianhua, Ye Youyin, et al. 2016. Phytoplankton community and environmental correlates in a coastal upwelling zone along western Taiwan Strait. Journal of Marine Systems, 154: 252–263, doi: 10.1016/j.jmarsys.2015.10.015

Wang Dongxiao, Shu Yeqiang, Xue Huijie, et al. 2014. Relative contributions of local wind and topography to the coastal upwelling intensity in the northern South China Sea. Journal of Geophysical Research: Oceans, 119(4): 2550–2567, doi: 10.1002/2013JC009172

Wang Daoru, Yang Yi, Wang Jia, et al. 2015. A modeling study of the effects of river runoff, tides, and surface wind-wave mixing on the eastern and western Hainan upwelling systems of the South China Sea, China. Ocean Dynamics, 65(8): 1143–1164, doi: 10.1007/s10236-015-0857-3

Wu Risheng, Li Li. 2003. Summarization of study on upwelling system in the South China Sea. Journal of Oceanography in Taiwan Strait (in Chinese), 22(2): 269–277

Xie Lingling, He Chaofeng, Li Mingming, et al. 2017. Response of sea surface temperature to Typhoon passages over the upwelling zone east of Hainan Island. Advances in Marine Science (in Chinese), 35(1): 8–19

Xie Shangping, Xie Qiang, Wang Dongxiao, et al. 2003. Summer upwelling in the South China Sea and its role in regional climate variations. Journal of Geophysical Research: Oceans, 108(C8): 3261, doi: 10.1029/2003JC001867

Xie Lingling, Zhang Shuwen, Zhao Hui. 2012. Overview of studies on Qiongdong upwelling. Journal of Tropical Oceanography (in Chinese), 31(4): 35–41

Xie Lingling, Zong Xiaolong, Yi Xiaofei, et al. 2016. The interannual variation and long-term trend of qiongdong upwelling. Oceanologia et Limnologia Sinica (in Chinese), 47(1): 43–51

Xu Jindian, Cai Shangzhan, Xuan Lili, et al. 2013. Study on coastal upwelling in eastern Hainan Island and western Guangdong in summer, 2006. Acta Oceanologica Sinica (in Chinese), 35(4): 11–18

Xue Yan, Kumar A. 2017. Evolution of the 2015/16 El Niño and historical perspective since 1979. Science China Earth Science, 60(9): 1572–1588, doi: 10.1007/s11430-016-0106-9

Yang Dezhou, Yin Baoshu, Sun Junchuan, et al. 2013. Numerical study on the origins and the forcing mechanism of the phosphate in upwelling areas off the coast of Zhejiang province, China in summer. Journal of Marine Systems, 123–124: 1–18, doi: 10.1016/j.jmarsys.2013.04.002

Yin Jianqiang, Huang Liangmin, Li Kaizhi, et al. 2011. Abundance distribution and seasonal variations of *Calanus sinicus* (Copepoda: Calanoida) in the northwest continental shelf of South China Sea. Continental Shelf Research, 31(14): 1447–1456, doi: 10.1016/j.csr.2011.06.010

Zeng Zhen, Chen Fajin, Meng Yafei, et al. 2015. Nutrient structure and its influence on phytoplankton growth in the Qiongdong Sea during winter and summer. Journal of Guangdong Ocean University (in Chinese), 35(3): 70–77

Zhai Hongchang, Ning Xiuren, Tang Xuexi, et al. 2011. Phytoplankton pigment patterns and community composition in the northern South China Sea during winter. Chinese Journal of Oceanology and Limnology, 29(2): 233–245, doi: 10.1007/s00343-011-0111-x